Iranian Journal of Science and Technology, Transactions of Civil Engineering (2023) 47:1007–1023
https://doi.org/10.1007/s40996-022-00936-4

RESEARCH PAPER

Seismic Performance Comparison of Fixed and Base-Isolated Models

Esra Ozer[1] · Mehmet Inel[1] · Bayram Tanik Cayci[1]

Received: 23 February 2022 / Accepted: 19 July 2022 / Published online: 2 August 2022
© The Author(s), under exclusive licence to Shiraz University 2022

Abstract
This study aims to compare seismic response of fixed-base and most preferred base isolation models including lead rubber bearing (LRB), curved surface friction bearing (FPS) and flat slider (FS) types for regular low- and mid-rise reinforced concrete (RC) framed buildings. For this purpose, 352 nonlinear time history analyses of three-dimensional building models were carried out considering 11 different ground motion pairs. Most important parameters related to seismic behavior of base-isolated systems such as displacement and acceleration demands, interstory drift ratios, base shear demands and isolator capacity usage ratios were investigated. The fixed-base models were subjected to the highest seismic demands as expected. While significant part of individual analysis cases exceeded controlled damage state for fixed-base models, only a few cases reached limited damage state in base-isolated models. Although total lateral displacement values are much higher for base-isolated models, significant part of seismic demands is damped at isolator interface and transmitted demands are at negligible level. Obtained results indicated that using LRB and FS type isolators together causes increase in seismic demands compared to the use of only LRB isolators since FS type isolators cannot generate recall force. LRB type isolators seem to be a better choice for regular buildings that have not re-centering problem. Significant variation under different ground motion records is also observed for all analysis case. For that reason, it has great importance to use sufficient number of ground motion records for proper seismic performance evaluation.

Keywords Base isolation · Lead rubber isolator · Friction pendulum isolator · Flat slider · Time history analysis

1 Introduction

Seismic base isolation is a design concept that is used to limit the damage caused by strong earthquakes or to improve the performance of the structures. Important facilities that contain valuable equipment like telecommunication centers or hospitals are needed to be used immediately after destructive earthquakes. Thus, base-isolated systems are necessity for these types of structures rather than a choice. The control of structural movements for isolated buildings is carried out with a specially designed interface at the level of isolators. The main function of seismic isolators is to reduce the transmission of seismic demands from ground to superstructure while providing sufficient stiffness at service load levels for wind and small earthquakes (Ceccoli et al. 1999; Erduran et al. 2011; Seranaj 2018). In addition, the building is removed from the destructive effects of the earthquake by extending the vibration period of the system (Ozmen et al. 2011; Deringol and Bilgin 2018).

The isolation systems usually consist of elastomeric or sliding bearings. Among the elastomeric isolator types used in practice, lead core rubber bearings (LRB) are widely used for their higher initial stiffness and energy dissipation capacity. In sliding bearings, curved surface friction bearings (FPS) are preferred because problems like permanent sliding or residual displacement in isolator bearings are prevented. In general, single type of base isolator systems is preferred to be used in applications. But flat sliders (FS) among sliding isolator can be also used together with rubber isolators to meet high tensile stresses.

LRB type isolator is an elastoplastic device, with a lead plug steel plate and rubber layers sequentially and on top of each other. Although the damage at the lead plug after the earthquake cannot be determined, the contribution of the lead plug in the damping of earthquake forces is apparent. It is also known to provide elastic rigidity to the system under wind or service loads (Ryan et al. 2005; Ozdemir

✉ Esra Ozer
esrao@pau.edu.tr

[1] Department of Civil Engineering, Pamukkale University, Denizli 20160, Turkey

and Bayhan 2015). In systems with FPS type isolators, on the other hand, the reaction forces to prevent movement in small demands such as service loads are formed by the friction coefficient of the curved surface. The pendulum like behavior, which is formed due to the geometric shape of the isolator, causes the system to behave more like a fixed-base support, until exceeding the reaction force due to friction. Although this feature causes significant acceleration demands at the beginning of the movement in the superstructure, it ensures that the system reaches the starting point at the end of the movement. Therefore, depending on the friction and loading speed, FPS type isolators have advantages and disadvantages compared to the LRB type isolators (NZSEE 2019).

On the other hand, flat sliding type isolators (FS) are also among the friction isolator bearing types, but unlike FPS type isolators, they have a flat sliding surface and do not increase the natural period of the system. The mechanism of FS isolators typically consists of a steel disc coated with low-friction polymer material that slides on a stainless steel lined base plate (Whittaker 2016). They limit the shear force transferred to the superstructure, and the bearing lateral force is simply equal to the friction force. As this type of isolator is not self-centering, they can be used as an element of the isolation system and require a complementary self-centering mechanism to prevent the permanent isolation system from displacement. They are always used with another bearing type (usually with elastomeric isolators) since they cannot generate any restoration force (Mokha et al. 1991). Although seismic codes allow for an ultimate tensile stress of up to 3 times the shear modulus of the isolator, rubber-type isolators generally cannot tolerate a tensile stress of this magnitude (Kelly 2003). The FPS type isolators also do not have tensile load capacity to meet (Naeim and Kelly 1999). For this reason, it is preferred to use flat slider (FS) isolator types at points that may be subjected to such a large tensile stress in the design of buildings with isolation (for example, shear walls and their surroundings) (Ghasemi and Talaeitaba 2020).

Design stage of base isolators is generally an iterative process, and there is not only one solution to meet design criteria such as maximum displacement value. Therefore, designers should find the optimum solution in case of cost and performance of system. For example, by changing the radius of curvature and the surface friction coefficient the behavior of the FPS isolator system could be further improved (Panchal 2009; Soni et al. 2011).

Previous research on the building response as a function of the isolator type revealed that elastomeric isolators (lead core rubber bearing (LRB)) take larger base displacements but transmit lower accelerations to the superstructure compared to friction pendulum isolator (FPS) (Jangid and Kelly 2001; Matsagar and Jangid 2004; Ordonez et al. 2003; Vaez et al. 2012). The large displacement problems of LRB type isolation system can be eliminated by applying significant damping (Sengel et al. 2009). In FPS type isolators with pendulum-like motion, permanent deformations in the system are reduced to a minimum; therefore, they are relatively insensitive to changes in input demands (Mokha et al. 1991; Zayas and Mahin 1987; Mazza and Mazza 2016; Mazza 2017).

Actual behavior of isolators deviates from numerical models since parameters like loading speed, heating, variability in production, pollution, cumulative movement, wear, aging, and environmental effects are idealized by using the simplified property modification factors in international seismic provisions or codes (FEMA-P-751 2012; FEMA-P-1051 2016; McVitty and Constantinou 2015; Eurocode-8 2005; AASHTO 2014;ASCE/SEI-7-16 2016; TBEC 2018). Considering the reduction in the probability of these effects occurring at the same time, lower and upper limits are determined with different combinations. The purpose of the lower and upper limit values derived from partially standardized prototype tests is to achieve a certain standard in production by keeping the average design value of each isolator within a certain range (Mazza and Mazza 2017; Mazza 2019; Gandelli et al. 2019; De Domenico 2019).

When previous applications about base isolator systems are considered, single type base isolation models are mostly preferred (Heaton 1995). However, in recent years like New de Young Museum in San Francisco, multiple type systems are also preferred in base-isolated building models (FEMA-P-752 2009). In general, LRB and FS type isolators are mostly preferred to be used together in multiple base-isolated models.

Although there are many studies in the literature (Kelly 2003; Almazán et al. 2002; Sharbatdar 2011) related with isolator systems and comparison with fixed-base models, limited number of these studies considers different type of base-isolated systems with using three-dimensional building models. The studies were conducted using either a few three-dimensional model (with or without infilll wall or soft story irregularity) or several two-dimensional models (Mazza et al. 2018, 2017; Wu and Samali 2002). Also, nonlinear behavior of superstructure models is mostly ignored due the assumption of significant decrement in transmitted seismic demands to the superstructure (Erduran et al. 2011; Mazza et al. 2018; Cancellara 2019). However, nonlinear behavior is possible to occur under intensive seismic demands even if significant plastic deformations at structural members are not expected. Another important point to be emphasized that frequency content of ground motion records directly affects seismic behavior of base-isolated models. To overcome these difficulties, sufficient number of ground motion records should be used in dynamic analysis (Ozmen 2017). When previous studies are evaluated, limited number of

ground motion sets or record in a specific region were used (Şengel et al. 2009; Kulkarni and Jangid 2002; Jangid 2007; Kilar and Koren 2009; Tena-Colunga and Escamilla-Cruz 2007).

This study aims to compare behavioral differences of fixed-base, LRB, FPS, and LRB + FS base isolator systems considering nonlinear behavior for three-dimensional low- and mid-rise reinforced concrete (RC) framed buildings. For this purpose, 3-, 5-, 7-, and 9-story RC building models without any structural irregularity were used. Nonlinear behavior of structural members and base isolators was also considered in dynamic analyses. Nonlinear time history analyses were performed using 11 different bi-directional ground motion pairs by applying two horizontal components, simultaneously to achieve a detailed investigation for dynamic response and comparison of fixed-base and base isolator systems.

2 Ground Motion Records

A total of 11 ground motion record sets which were selected from the PEER Ground Motion Database of the Pacific Earthquake Engineering Research Center (PEER 2019) were used for the time history analyses. Horizontal components of each record were scaled according to the elastic acceleration spectrum for 5% elastic damping ratio defined in TBEC-2018 (2018). Scaling process was conducted using spectral matching, which is the most recommended earthquake record selection method for seismic codes (Kayhan et al. 2011; Ozmen et al. 2019).

The spectral matching process is carried out for the $0.2T_p$-$1.5T_p$ ranges for the fixed-base models and $0.5T_M$-$1.25T_M$ for the base-isolated models, respectively. The periods of building models are in the limit values of these intervals. Therefore, a single spectral matching process was carried out for both fixed-base and base-isolated models.

The spectral parameters used for the building location are given in Table 1 for the design earthquake with 10% probability of exceedance in 50 years. In the table, the short-period design spectral acceleration coefficient and the design spectral acceleration coefficient for the 1.0 s period are expressed as S_{DS} and S_{D1}, similar to S_{MS}, S_{M1} of FEMA-P-1051 (2016), respectively. The short-period map spectral acceleration coefficient and the map spectral acceleration coefficient for the 1.0 s period are expressed as S_S and S_1, respectively.

Comparisons of elastic acceleration spectrums are illustrated in Fig. 1 for the 5% damping ratio for the selected records. In addition, the spectrum of TBEC-2018 on the ZC soil type with a probability of exceeding 10% in 50 years and the average spectral acceleration of the ground motion records were plotted on the same figure. Although the scatter of the selected records is high, the average values are very close to the TBEC-2018 spectrum requirement (1.3 times design spectrum). The properties of the ground motion records used are given in Table 2.

Table 1 Spectral parameters of design earthquake level (DD-2) for building location (TERM 2018)

Parameters	Value
S_1	0.261
S_S	1.135
S_{D1}	0.658
S_{DS}	1.135

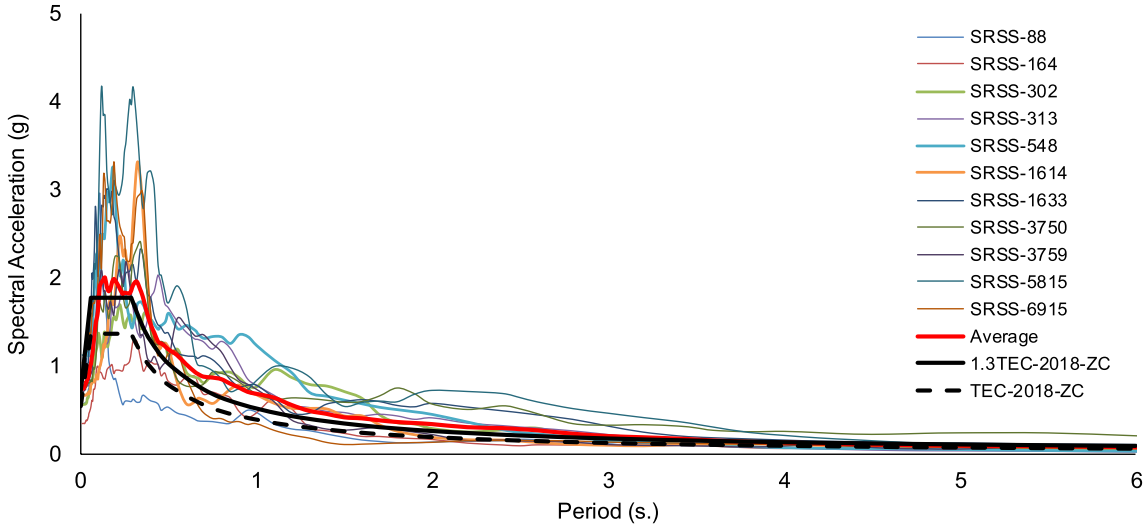


Fig. 1 Elastic acceleration spectrum of the scaled records for 5% damping

Table 2 Ground motion database used for the study (TERM 2018)

No	RSN	Earthquake	Year	Location	Mw	Component H_1s–H_2	PGA (g)	Vs30 (m/s)	Scale factor
1	88	San Fernando	1971	Santa Felita Dam	6.6	000–090	0.387	389.0	2.5
2	164	Imperial Valley-06	1979	Cerro Prieto	6.5	000–090	0.252	471.5	1.5
3	302	Irpinia_ Italy-02	1980	Rionero In Vulture	6.2	000–270	0.399	574.9	4.0
4	313	Corinth_ Greece	1981	Corinth	6.6	000–090	0.592	361.4	2.0
5	548	Chalfant Valley-02	1986	Benton	6.2	270–360	0.733	370.9	3.5
6	1614	Duzce_ Turkey	1999	Lamont 1061	7.1	E-N	0.525	481.0	4.0
7	1633	Manjil_ Iran	1990	Abbar	7.4	000–090	0.617	724.0	1.2
8	3750	Cape Mendocino	1992	Loleta Fire Station	7.0	270–360	0.531	515.7	2.0
9	3759	Landers	1992	Whitewater T.Farm	7.3	180–270	0.494	425.0	4.0
10	5815	Iwate_ Japan	2008	Yuzawa	6.9	EW-NS	0.791	655.5	4.0
11	6915	Darfield_ N.Zealand	2010	Heathcote V. PS	7.0	000–090	0.930	422.0	1.2

3 Modeling

3.1 Fixed-Base Models

This study considers four different 3D reinforced concrete (RC) building models to represent low- and mid-rise building stock. For this purpose, 3-, 5-, 7-, and 9-story buildings with fixed-base assumption were designed according to 2018 Turkish Building Earthquake Code (TBEC 2018) for life safety performance level. In building design, elastic design spectrum with a return period of 475 years corresponding to DD2 level seismic demands in TBEC-2018 is considered. The building models are symmetrical for both orthogonal axes without any structural irregularity. They are RC framed buildings without shear walls. Plan view of the building models is shown in Fig. 2. Typical story heights are 3.2 m throughout the building height. Compressive strength of concrete and yield strength of steel values are assumed to be 30 and 420 MPa, respectively. The considered buildings are assumed to be located on soil type ZC defined in TBEC-2018 which is similar to soil type C in FEMA-450 (FEMA-P-450 2003) for the design purposes.

Nonlinear behavior of structural members was reflected by user-defined plastic hinges by defining at both ends of beams and columns. Moment–curvature diagrams of beam and column members were obtained by considering the dimensions, longitudinal and transverse reinforcement contents, and axial load levels of RC members using SEMAp software (SEMAp 2008). Rotation values required for the nonlinear analyses were defined in the SAP2000 program used in the modeling and analysis stages (SAP2000 2020). Plastic hinges at column members were applied considering M2-M3 interaction since time history analyses performed as bi-directional. The effective section stiffness of column and beam members were defined 0.70EI and 0.35EI as defined in TBEC-2018, respectively (TBEC 2018; Ozer et al. 2022). The column and beam dimensions and dynamic properties (period—T, seismic weight—W, and base shear force—V_t) of the used building models are provided in Table 3. Section properties of structural members are the same throughout the building height.

3.2 Base-Isolated Models

The base isolators were placed at the base of each column members for the 3-, 5-, 7-, and 9-story models. Three different base-isolated cases were considered as only LRB, only FPS and both LRB and FS (LRB + FS) in the scope of this study. The isolators with different stiffness values were placed symmetrically according to plan geometry for LRB + FS models. In this way, the center of mass of the superstructure and the center of stiffness of all isolated building models coincide to prevent a possible torsional irregularity.

Illustration of LRB type base isolator model is given in Fig. 3a. Idealized bi-linear hysteretic behavior of the LRB isolator is shown in Fig. 3b. The parameters on the figure are characteristic strength (F_Q), initial (elastic) rigidity (k_1), secondary (inelastic) rigidity (k_2), effective stiffness (k_e) corresponding to the horizontal force (F) and isolator displacement (D), effective yield strength (F_y), and effective yield displacement (D_y).

Stability and overturning conditions under static and earthquake loading are required to be met during iterative design process of the LRB type isolator. These conditions are given in Fig. 4 and Eqs. (1)-(3). Parameters of t, P, Δc, F, Δs, M, and θ correspond to height of each rubber layer, axial force, vertical displacement due to axial force, lateral force, horizontal displacement due to lateral force, moment, and rotation, respectively. The terms, γ_{sc}, γ_{eq}, and γ_{sr} are compressive strain, strain due to lateral displacement, and rotational strain, respectively.

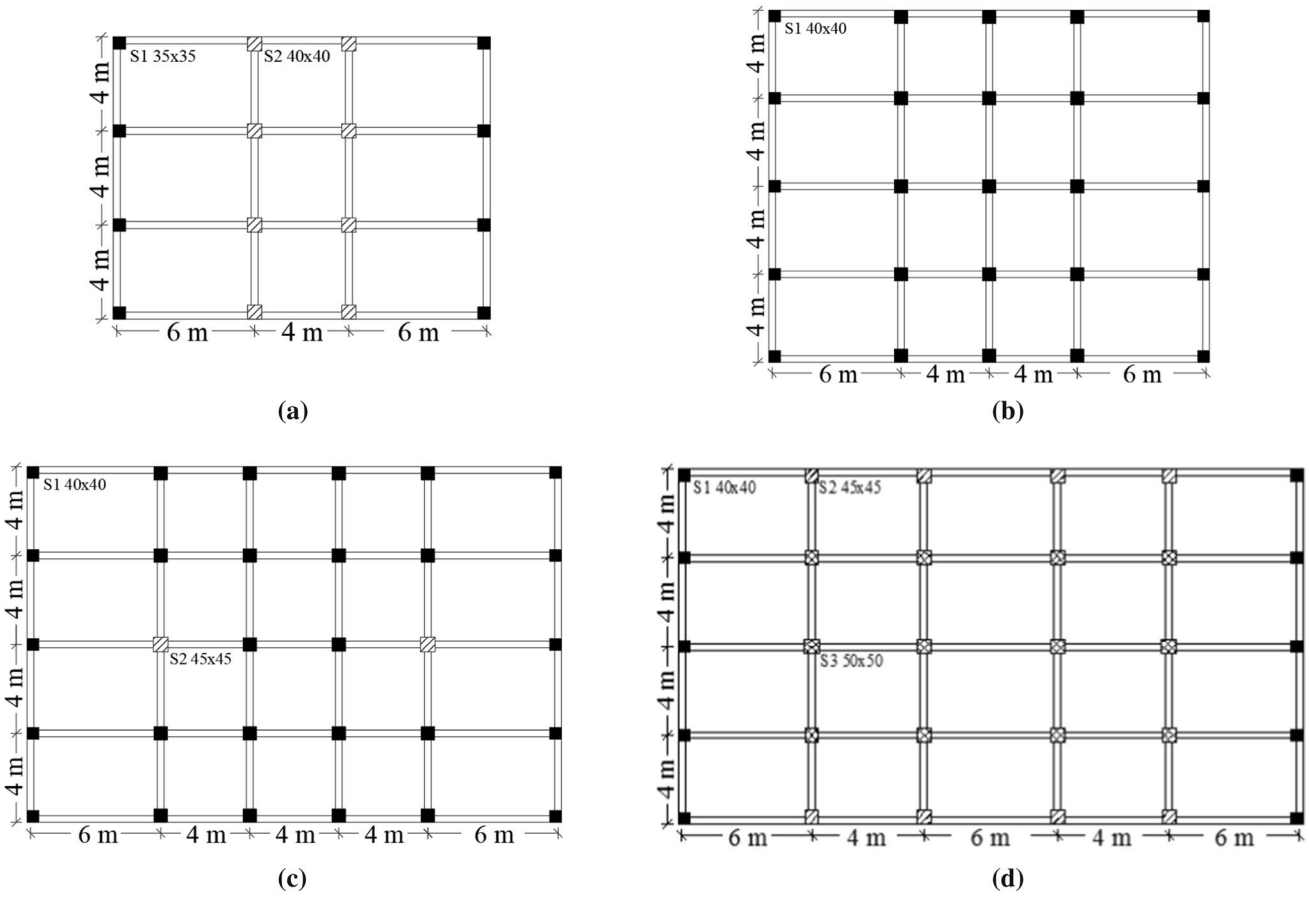


Fig. 2 Typical RC frame building plan views **a** 3-story, **b** 5-story, **c** 7-story, **d** 9-story

Table 3 Column and beam dimensions used in the RC framed buildings

Model	3-Story	5-Story	7-Story	9-Story
Beam elements (mm × mm)	300 × 500	300 × 500	300 × 500	300 × 500
Column elements (mm × mm)	350 × 350 400 × 400	400 × 400	400 × 400 450 × 450	400 × 400 450 × 450 500 × 500
T_x (s)	0.51	0.87	1.15	1.51
T_y (s)	0.48	0.82	1.12	1.34
T_z (s)	0.47	0.78	1.05	1.32
W (kN)	4623.6	12,753.8	19,885.5	32,623.2
V_{tx} (kN)	1549.8	3200	3472.6	4836.1
V_{ty} (kN)	1399.7	2996.7	3009.6	4565.2

$$\gamma_{sc} + \gamma_{eq} + \gamma_{sr} \leq 5.0 \quad (1)$$

$$\gamma_{sc} + \gamma_{eq} + \gamma_{sr} < 0.75\varepsilon_b \quad (2)$$

$$\gamma_{sc} + \gamma_{eq} + 0.5\gamma_{sr} \leq 6.0 \quad (3)$$

Parts and hysteretic behavior of a typical FPS type isolator is illustrated in Fig. 5. Unlike the hysteretic behavior of the LRB isolator, F_Q and F_y are equal and correspond to multiply to the effective friction coefficient (μ) and vertical force (P) acting on the isolation unit. Besides, the values of k_2 and k_e depend on the effective radius of curvature (R) of the curved frictional isolation unit sliding surfaces (Ozer et al. 2022).

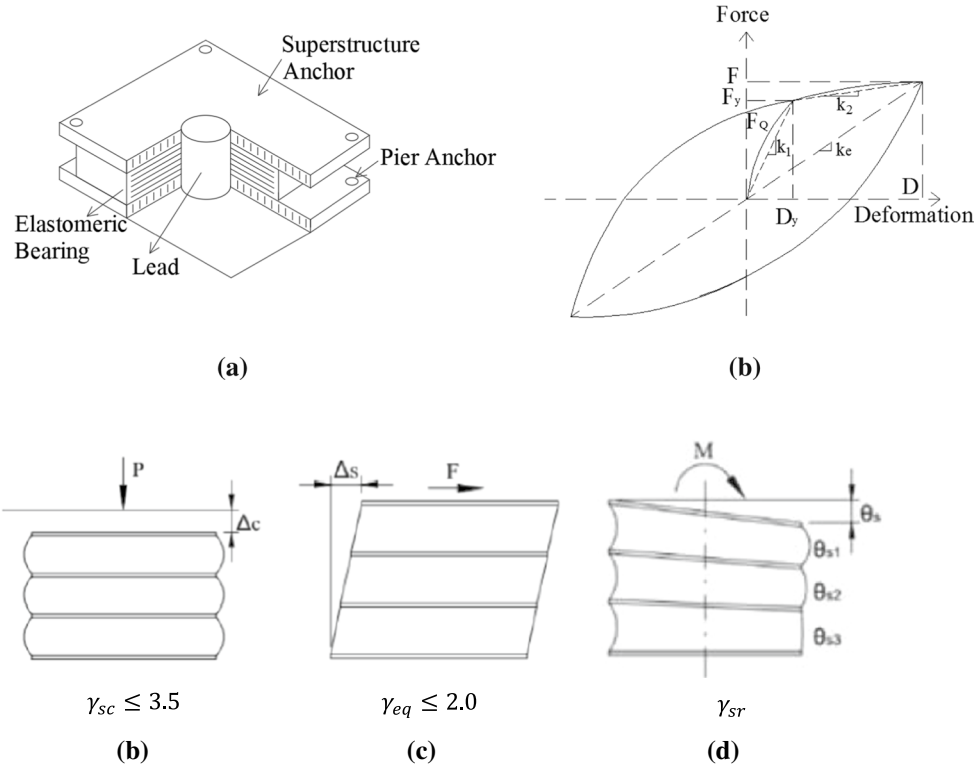


Fig. 3 Lead rubber bearing isolator **a** its components and **b** its idealized hysteresis model (TBEC 2018)

Fig. 4 Unit strain of lead rubber bearing isolator **a** non-strain, **b** pressure force, **c** horizontal displacement except earthquake effect, **d** the relative rotation between the plates

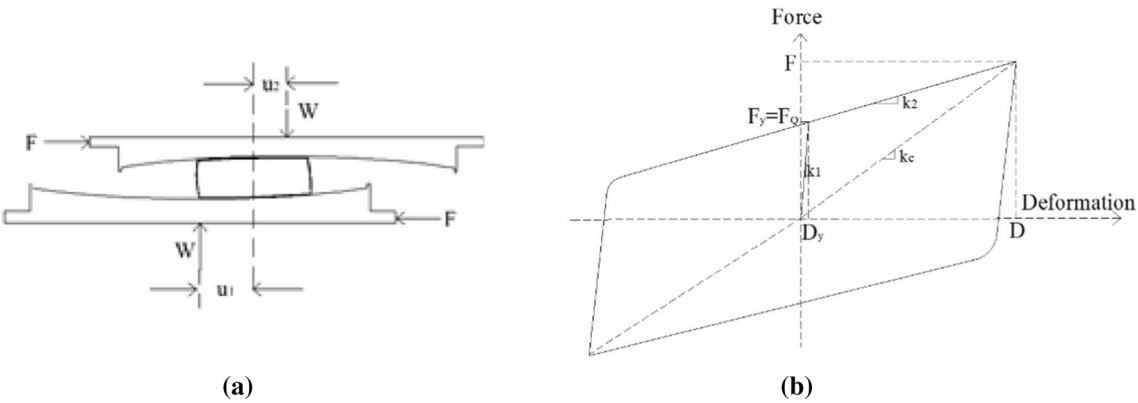


Fig. 5 Typical curved surface friction pendulum isolator **a** its components and **b** its idealized hysteresis model (TBEC 2018)

The hysteric loop given in Fig. 5 is idealized with the assumptions made in developing the mathematical model (e.g., constant consideration of the coefficient of friction, neglecting stick–slip behavior when the direction of motion changes). It is well known that there are many factors affecting the friction coefficient in real behavior such as sliding velocity, pressure (axial force), surface temperature of isolator, and deviation from idealized behavior (Mazza and Mazza 2017; Gandelli et al. 2019; De Domenico et al. 2019; Constantinou et al. 2007; Lomiento et al. 2012). Since it is not possible to define actual hysteretic loop in modeling, an idealized bi-linear hysteretic loop is used for modeling purposes as defined in FEMA-451B (2016).

Typical view of FS type base isolator model and its hysteretic behavior is shown in Fig. 6. Unlike the FPS type isolator, the effective radius of curvature is infinite ($R \rightarrow \infty$) and its post-yield stiffness (k_2) is equal to zero. In addition,

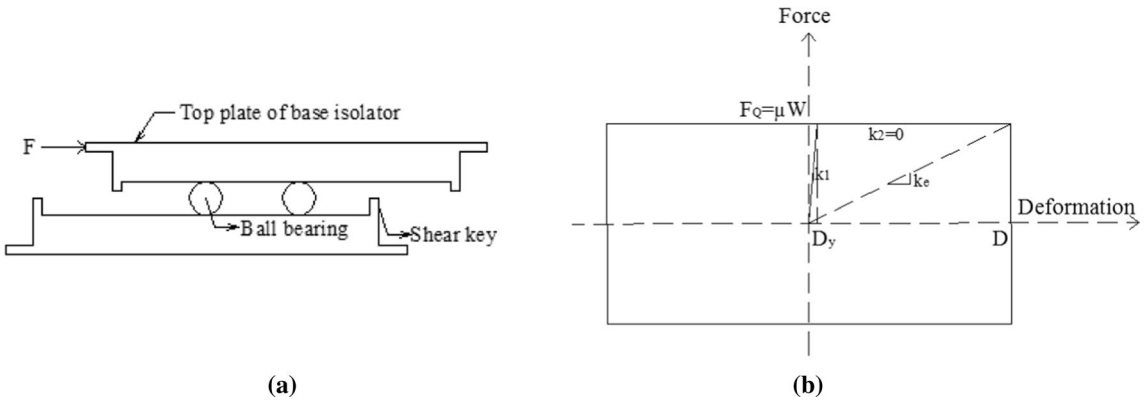


Fig. 6 Flat slider isolator **a** parts and **b** its hysteresis model

bearing lateral force is simply equal to the friction force of surface.

The design parameters of the isolators used in this study are summarized in Table 4. k_v and ξ_{eff} are the stiffness in the vertical direction and effective damping, respectively. These parameters were determined by considering maximum design displacement value (D_{max}) given in the table. In the scope of this study D_{max} value is assumed equal to minimum allowable displacement value defined in TBEC-2018 (TBEC 2018; Ozer et al. 2022). Additionally, the modal ratios are assumed to 0% in isolation modes (first three modes) and 2% non-isolated /structural modes, respectively (Giammona et al. 2015; Hall 2006; Ryan and Polanco 2008).

When flat sliding and rubber isolators are used together in models, the sharing of superstructure weight between isolators should be determined. International practices seem to

Table 4 Design parameters of the used LRB, FPS, and FS type isolators

Parameters	Unit	3-Story LRB	5-Story LRB	7-Story LRB	9-Story LRB
k_v	kN/m	98,399	186,035	192,520	440,057
k_e	kN/m	143	305	294	252
k_2	kN/m	98	209	202	173
F_y	kN	14.7	31.3	34.2	39.7
k_2/k_1	–	0.69	0.54	0.50	0.46
ξ_{eff}	–	0.15	0.20	0.22	0.25
D_{max}	m	0.35	0.40	0.40	0.45
Parameters	Unit	3-Story FPS	5-Story FPS	7-Story FPS	9-Story FPS
k_e	kN/m	99	445	622	676
k_2	kN/m	76	99	85	124
μ	–	0.03	0.03	0.03	0.03
R	m	2.24	2.24	3.05	4.24
ξ_{eff}	–	0.20	0.24	0.27	0.29
D_{max}	m	0.35	0.40	0.40	0.45
Parameters	Unit	3-Story FS	5-Story FS	7-Story FS	9-Story FS
k_e	kN/m	10E + 10	10E + 10	10E + 10	10E + 10
k_2	kN/m	0	0	0	0
μ	–	0.08	0.08	0.08	0.08
R	m	∞	∞	∞	∞
D_{max}	m	0.35	0.40	0.40	0.45

allow only a small fraction of the superstructure weight to be supported on flat sliding isolators since the more weight on sliders, the more variable the isolator performance (NZSEE 2019; FEMA-P-752 2013). Therefore, the function of flat sliding isolators is to manage the post-elastic stiffness of system. In the study conducted by Whittaker, it was stated that the axial load ratio of flat sliding isolators may be determined as much as 2/3 of the building weight (Whittaker 2016).

As shown in Table 4, stiffness parameters of each type of isolators are different. Thus, it has great importance to manage the placement and ratio of different type base isolators in system. This is an iterative process, and different combinations can be derived that ensure the target stiffness level and target displacement value of system. The improper placement of isolators may result in undesirable irregularities such as torsional behavior. In this study, placement of FS type isolators is determined in a way that no torsional behavior occurred in the dominant vibration mode for both directions. In addition, the maximum number of FS type isolator were used to meet the system period value of at least 3 times the fixed-base model period. In Fig. 7, plan view of the models with FS and LRB type isolators used together is given.

4 Results and Discussion

A detailed comparison was carried out for fixed-base and base-isolated models subjected to 11 pairs of spectrum compatible record sets. A total of 352 different nonlinear time history analyses were carried out for 16 different models (fixed-base, only LRB, only FPS and LRB + FS base isolator systems of 3-, 5-, 7- and 9-story buildings). The same target displacement values were used at design stage of all isolated building models for proper evaluation of behavioral differences of different type base isolator models. Many parameters like relative and absolute displacement demands, interstory drift ratios, capacity/demand ratios of isolators, absolute acceleration values transmitted to superstructures, and base shear demands are obtained and compared in the scope of this study.

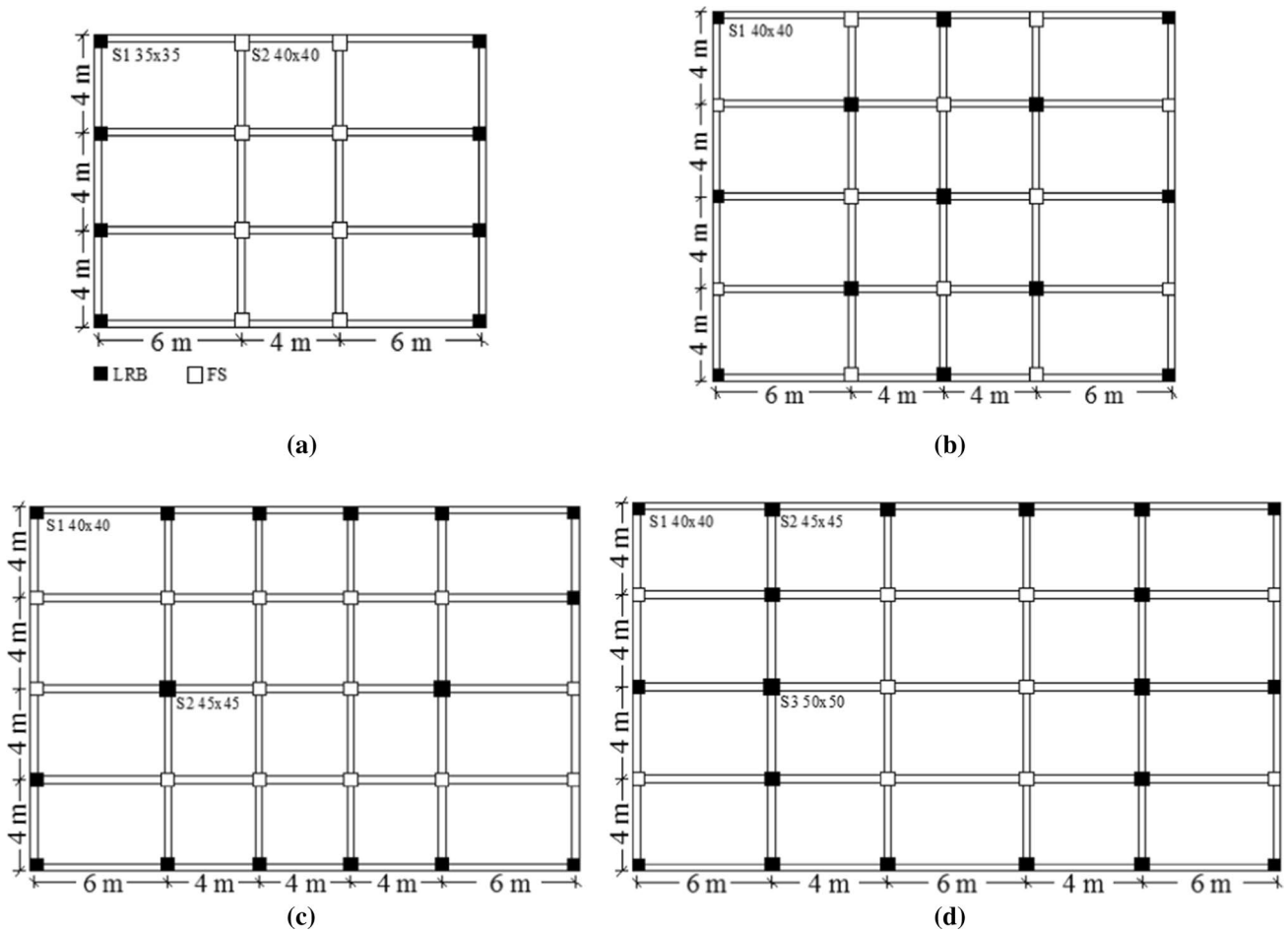


Fig. 7 LRB and FS type isolator location of the considered LRB + FS buildings **a** 3-story, **b** 5-story, **c** 7-story, **d** 9-story

The isolated building model-dominant periods are summarized in Table 5. The increase in period values is obvious for base-isolated systems compared to fixed-base models. FPS type base-isolated models tend to have lower vibration periods compared to the LRB type base-isolated models. This is related that FPS type isolators have higher effective stiffness values for same design displacement values compared to LRB type isolators. Since the same isolators of the LRB model were used and there is no contribution to period from the flat sliding isolators, the period values of LRB + FS models are less than the LRB models.

The hysteretic cycles in the base-isolated models are affected by frequency content and characteristics of the earthquake and design properties of the isolator. Besides, LRB, FPS, and FS type isolators have different hysteretic cycle characteristics due to behavioral differences. Hysteretic cycles of LRB, FPS, and FS type isolators under RSN-5815 record are illustrated in Fig. 8 as an example. The area of the hysteretic loop is an indicator of the energy dissipated by the isolator and provides a general impression of the designed isolator about its initial and post-yielding stiffnesses, etc.

Table 5 Comparisons of model parameters

Model		3-story	5-story	7-story	9-story
LRB	T_x (s)	2.98	3.34	5.01	5.51
	T_y (s)	2.36	3.32	4.84	5.18
	T_z (s)	1.95	3.15	4.24	4.87
FPS	T_x (s)	2.58	3.03	4.05	4.82
	T_y (s)	2.01	2.94	3.62	4.02
	T_z (s)	1.69	2.37	2.97	3.61
LRB + FS	T_x (s)	2.38	2.75	3.77	4.95
	T_y (s)	2.12	2.67	3.35	4.02
	T_z (s)	1.71	2.25	2.98	3.55

4.1 Evaluation of Displacement Demands

The maximum roof displacement demands of the building models subjected to the ground motion records are obtained using nonlinear time history analyses. Figure 9 shows comparisons of roof displacement demand history according to ground (Fig. 9a) and isolator interface (Fig. 9b) for fixed-base and base-isolated systems under the RSN-5815 ground motion record of the 5-story building model, to illustrate the behavioral differences as an example. It is obvious that the displacement history of the fixed-base model significantly deviates from the base-isolated models, while the demands transferred to the superstructure are negligible after the earthquake demands are damped at the isolator interface (Fig. 9b). While permanent displacements due to excessive plastic deformations are clearly observed for fixed-base model, the base-isolated models do not have any permanent displacement. Also, lateral displacement demands occurred at super-structure are considerably lower for LRB type isolator system compared to FPS and LRB + FS type isolator systems.

The roof displacement values are normalized to building heights to obtain roof drift ratios (RDR) which are plotted in Fig. 10. Both roof drift values with respect to ground and isolator interface are provided in the figure with "-g" and "-i" extensions, respectively. The figure shows that the displacement demands in fixed-base models are considerably higher than transferred superstructure displacement demands of base-isolated models. When roof drift demands are compared according to the ground level, total displacements of base-isolated models are much higher than fixed-base models as expected. The higher values of lateral displacements are inevitable for base-isolated models due to the vibration period increment of system. However, demands are mostly damped at the isolator interface, and the transferred demands to the

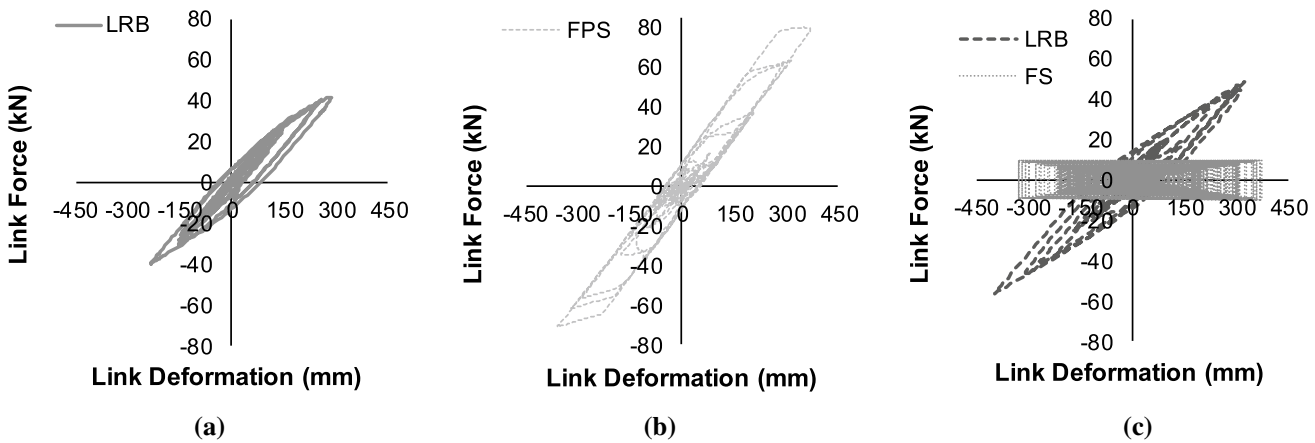


Fig. 8 Hysteretic cycles of models with sevenfold isolators according to isolator types for RSN-5815 record

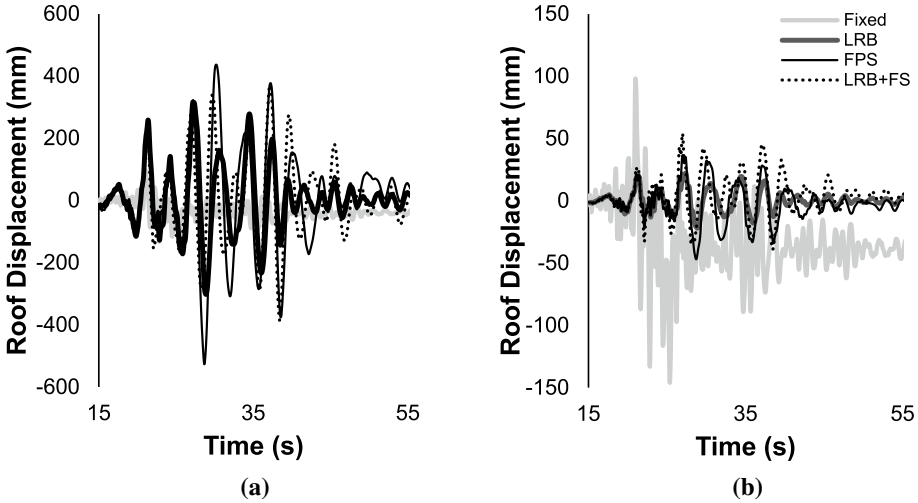


Fig. 9 Roof displacement of fixed and base-isolated building models subjected to the RSN-5815 ground motion record **a** absolute, **b** relative

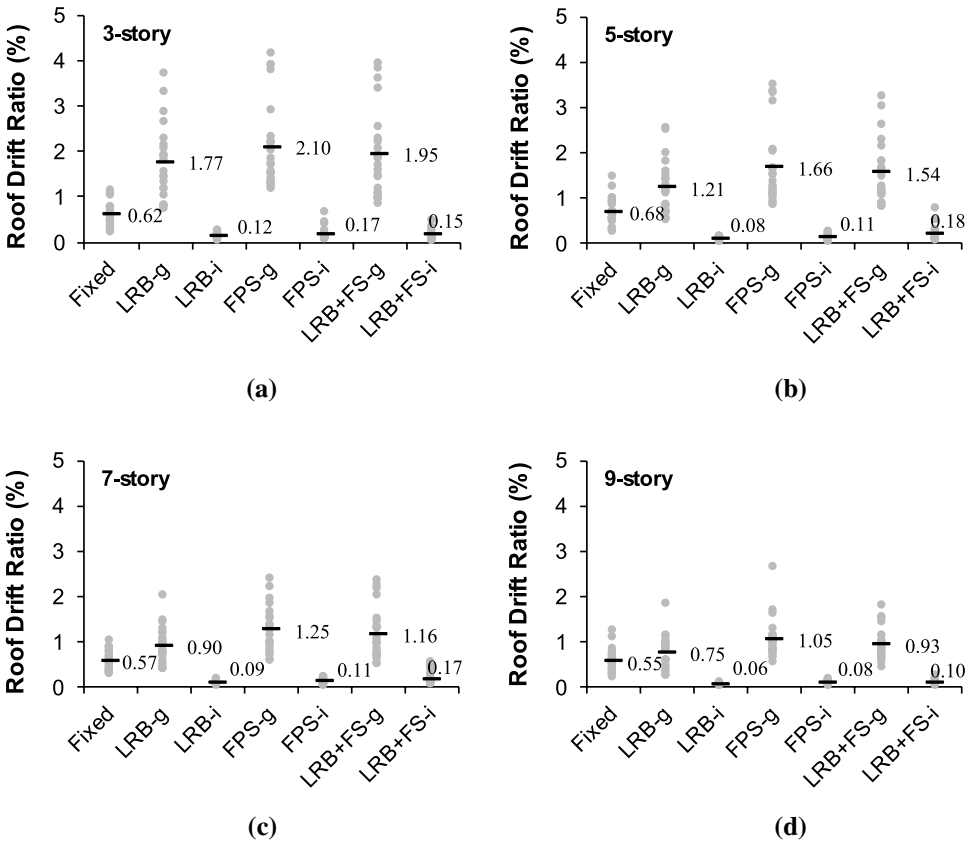


Fig. 10 Roof drift ratios of base-isolated building models subjected to the scaled ground motion set **a** 3-story, **b** 5-story, **c** 7-story, **d** 9-story

superstructure significantly decrease. Moreover, although there is no meaningful difference, the roof drift demands of LRB models with respect to ground or isolator level are slightly lower compared to that of FPS and LRB + FS models. Since FS type isolators cannot generate recall force and movements are prevented by relatively small friction coefficient, the highest transferred superstructure displacement demands are generally observed in LRB + FS models.

The obtained results indicate that significant scatter exists in displacement demands of individual ground motion records for all models. Similar to the previous studies, it is observed that frequency content of ground motion records affects the dynamic response of the base-isolated system (Guner 2012; Matsagar and Jangid 2010; Tena-Colunga and Zambrana-Rojas 2006). The scatter observed in Fig. 10 illustrates that FPS and LRB + FS type isolators are more sensitive to the frequency content effect.

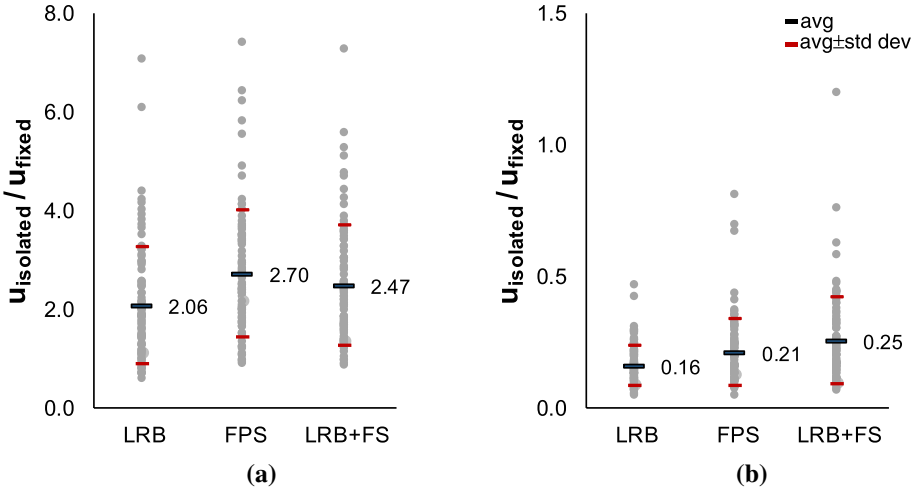


Fig. 11 Ratio of average roof displacement demands of isolated systems to the average roof displacement of fixed base for all buildings with respect to **a** ground and **b** isolator interface

The average RDR ratios for isolated/fixed-base models are given in Fig. 11. Displacement demands with respect to the ground are at least two times higher for all base-isolated models. The difference of total displacement demand ratios is increased up to 8 times in FPS type isolators as observed in previous studies (Erduran 2011; Ismail 2015; Meral 2021). However, significant part of displacement demands is absorbed at the isolator interface. Therefore, the displacement demands transferred to the superstructure are relatively small in the base-isolated models. The lowest superstructure displacement demand is observed as 16% of fixed-base model demand for LRB type isolators. These ratios are 21% and 25% for FPS and LRB + FS type isolators, respectively.

The ratio of the maximum displacement demands at base isolator level and total displacement demands at roof level is given in Fig. 12. Since all building models show similar trend, their average values are plotted on the same figure. It is obvious that more than 90% of displacement demands are at the isolator system regardless of the isolator type. Although lateral stiffness values of LRB, FPS, and LRP + FS type isolators are significantly different, these values have limited effect on the isolator displacement demands. Besides, it is apparent that the base-isolated systems are considerably effective to decrease the superstructure displacement demands subjected to ground motion records.

The average usage rate of the isolator lateral displacement capacity is given in Fig. 13. The average usage capacities are calculated as 45.0%, 58.1%, and 53.2% for LRB, FPS, and LRB + FS type isolators, respectively. Although displacement capacity of isolators is the same for each building model, lowest usage rate is observed with LRB type isolators due to their higher inelastic stiffness capacity compared to FPS and LRB + FS type isolators. However, individual analysis cases scatter in a large band and standard deviation value is very high. It is also observed that isolator usage

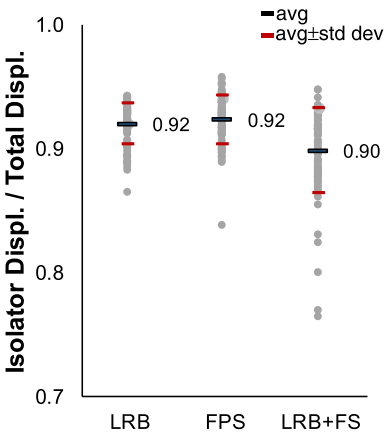


Fig. 12 Ratio of isolator displacements to the total displacements

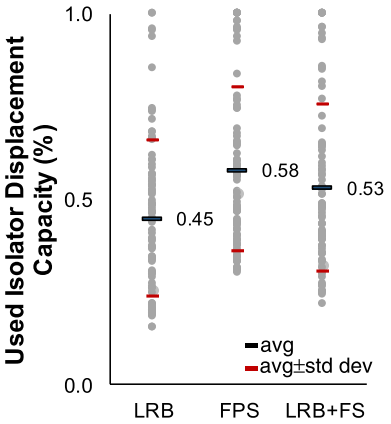


Fig. 13 Comparisons of isolator capacity usage ratios

rates are close to lateral displacement capacity for some of ground motion records. Therefore, the evaluation based on average values might be misleading. However, none of

analyses exceed the isolator displacement capacity which is quite expected since it is not allowed in design stage.

4.2 Evaluation of IDR Demands

Interstory drift ratio (IDR) is recognized as an important damage indicator to evaluate the change in displacement demands along to height of superstructures. The interstory displacement demands are normalized by story height, and obtained results are given in Fig. 14. Damage limit levels according to TBEC-2018 (2018) are also illustrated on the figure as "UU," "LD," "CD," and "C" abbreviations corresponding to uninterrupted use, limited damage, controlled damage, and collapse, respectively. The IDR profiles along the height are also compared in Fig. 15 to evaluate the difference in maximum IDR values between building models.

When the IDR values are examined, it is observed that all base-isolated models are at uninterrupted use (UU) performance level for both averages and each ground motion record. Although LRB type isolator models calculate smaller IDR demands compared to FPS and LRB + FS type isolator models, the difference is negligible. Since friction-based isolators behave as rigid as fixed-base models until lateral seismic forces exceed friction coefficient (Mazza et al. 2017), the larger IDR demands in the friction-based FS and FPS type isolators are observed compared to LRB type isolators. The IDR values for fixed-base models are significantly higher compared to base-isolated models as observed in previous studies (Erduran 2011; Yao and Li 2012). Average values are between 0.86% and 1.19%, and these values are almost 5 times higher than the IDR values of base-isolated models. Even the design of buildings was carried out according to controlled damage performance level, it is exceeded for limited number of ground motion records for all fixed-base models. By the nature of dynamic analysis, the marginal results are expected. The IDR profiles of fixed-base buildings are also significantly different from base-isolated models. The use of base isolation systems makes the IDR almost uniform, reducing the values down to the undamaged range.

4.3 Evaluation of Acceleration Demands

The maximum absolute acceleration values transmitted to the superstructure are another important parameter to evaluate seismic behavior of base-isolated models. Maximum absolute acceleration demands are calculated for each model, and average values along the height of structure are given in Fig. 16. The difference between fixed-base models and isolated models is calculated as 70.9% (LRB + FS) and 84.7% (LRB) based on average values. In addition, as observed in IDR demands, distribution of absolute acceleration demands of the fixed-base models is quite variable along the height, while the absolute acceleration values are almost uniform throughout the building height for base-isolated models. The maximum absolute acceleration demands

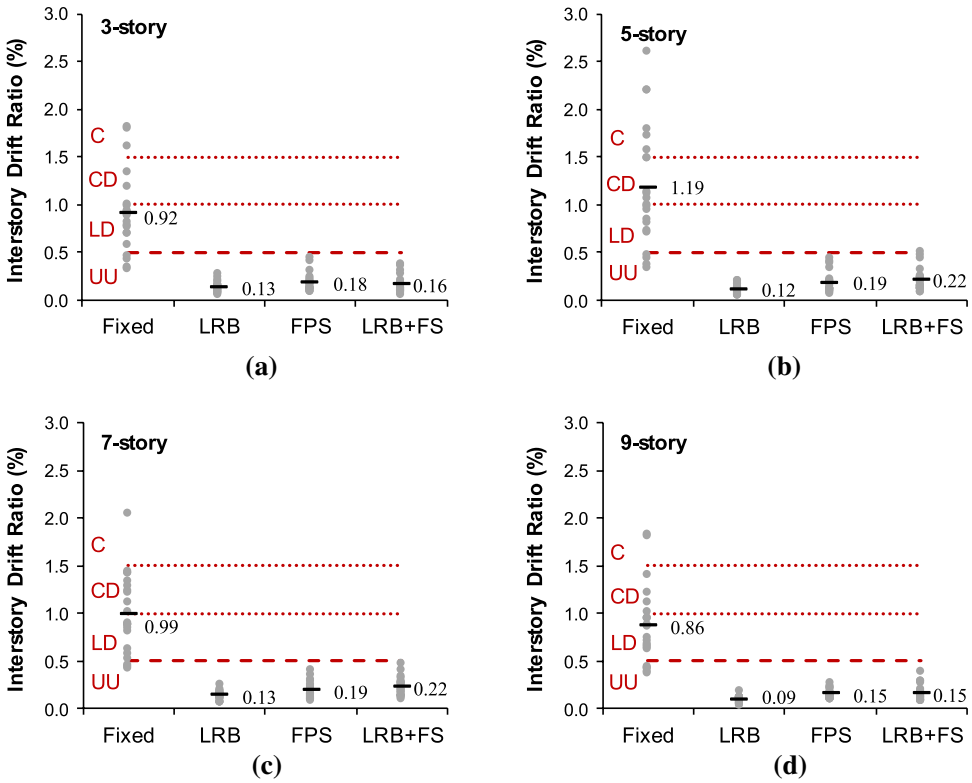


Fig. 14 Maximum interstory drift ratios (IDR) for the building models

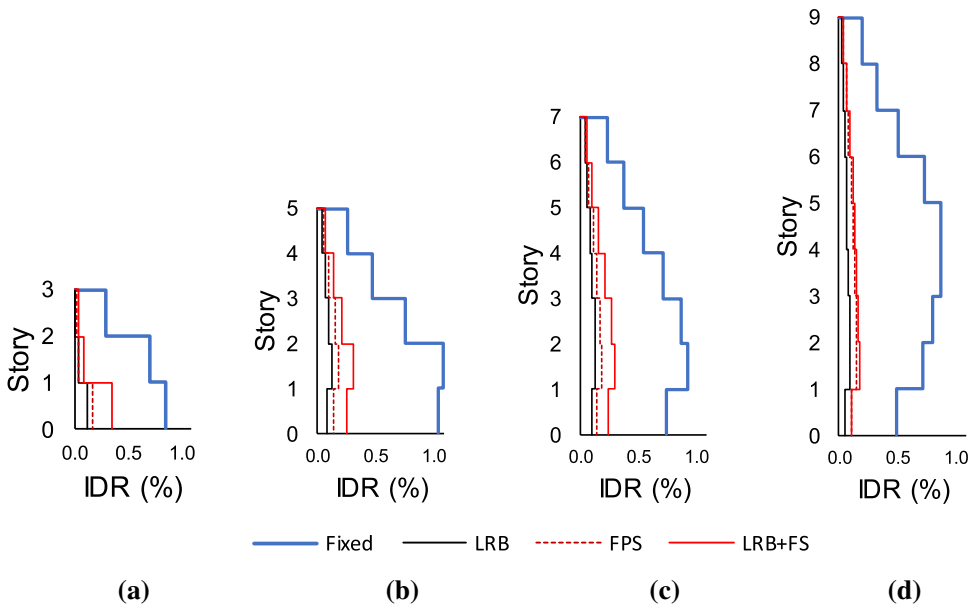


Fig. 15 Average maximum IDR profiles of models

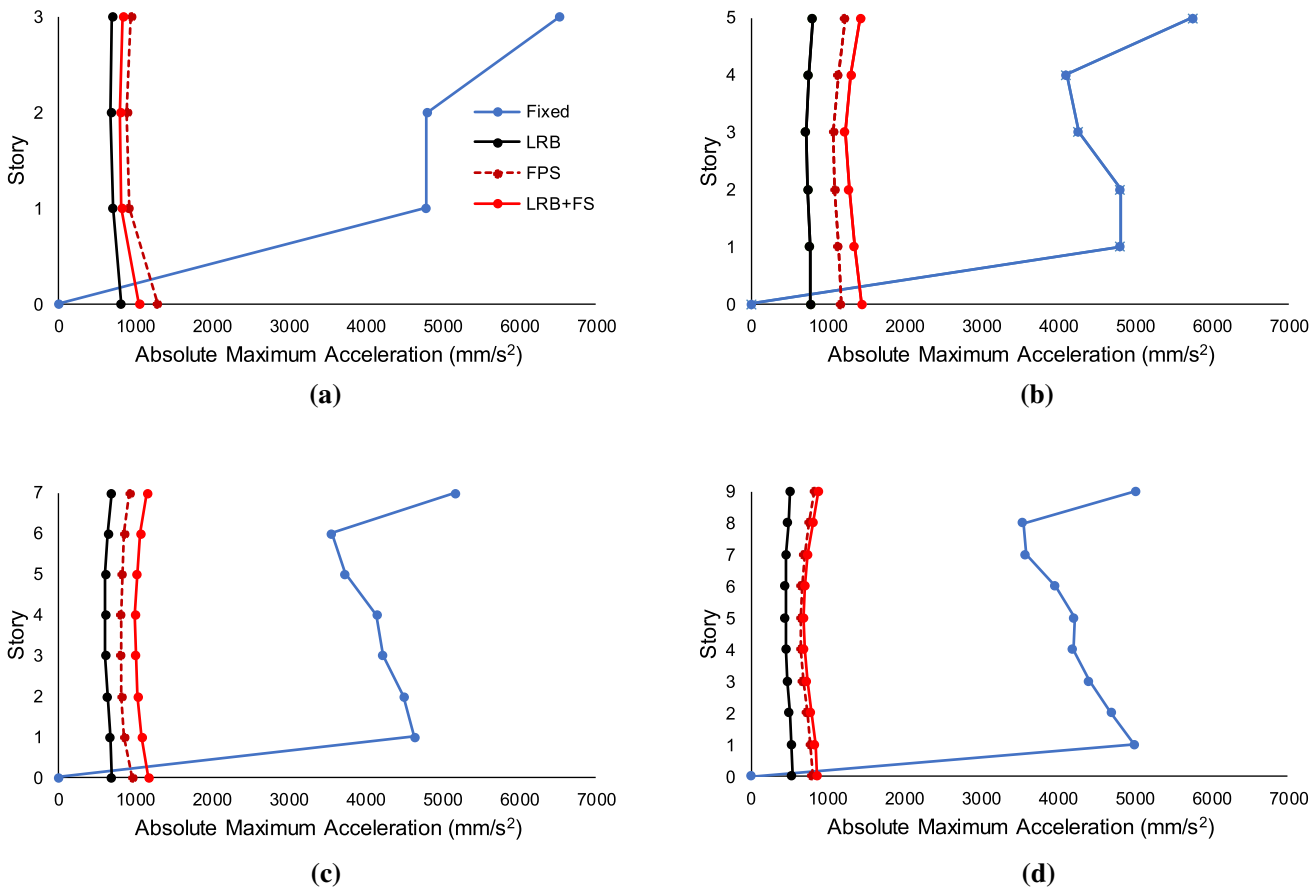


Fig. 16 Average maximum acceleration profile for models

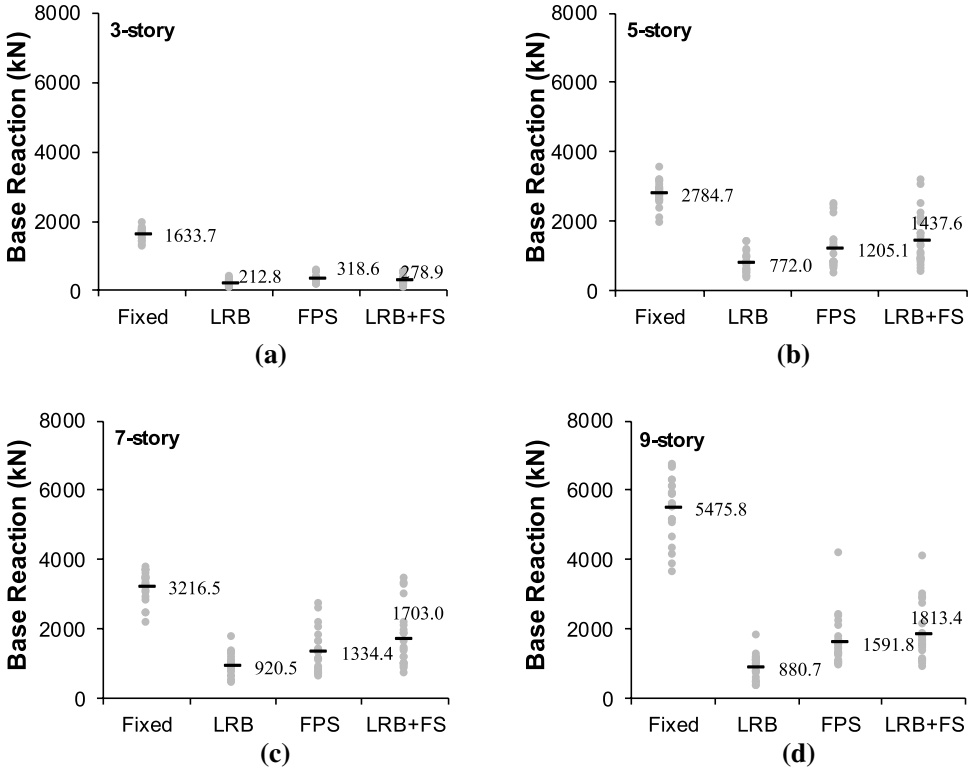


Fig. 17 Base reaction demands for all models

are higher in FPS and LRB + FS type models compared to the demands of LRB type models.

4.4 Evaluation of Base Reaction

The base shear force is another important parameter in evaluating the behavioral differences between the fixed-base and base-isolated models. The greater the level of shear force acting on the building, the higher the horizontal force distributed over the stories. The comparison of maximum base shear demands is illustrated in Fig. 17. The ratio of maximum base shear forces of base-isolated models to the fixed-base models is also given in Fig. 18.

The base shear demand trends are similar to other demand parameters evaluated in the scope of this study. The highest base shear force demands are calculated for fixed-base models (Ghasemi and Talaeitaba 2020; Ismail 2015; Yao and Li 2012). The difference between LRB and LRB + FS type isolators is apparent for all models. While base reaction force has decreased by at least 47.1% in LRB + FS type isolators, the decrease is up to 87% in LRB type isolators compared to fixed-base models. LRB + FS isolators have considerably lower lateral stiffness due to lack of restoring force capacity of FS type isolators (Mazza et al. 2018). For this reason, LRB type isolators are effective in reducing the base shear forces. When the base shear force ratios of base-isolated and fixed-base models are compared, the lowest decrease is observed in LRB + FS models as 62% while the highest decrease is 79% for LRB models (Fig. 18).

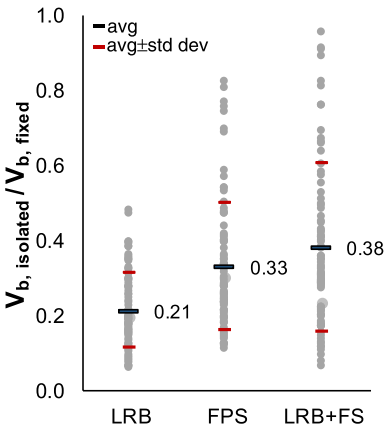


Fig. 18 Base shear reaction ratios of base-isolated and fixed-base models in average

5 Conclusions

This study investigates the behavioral differences of fixed-base assumption and most preferred base isolation models including LRB, FPS, and LRB + FS types for regular low- and mid-rise RC buildings. Three-dimensional modeling and nonlinear behavior of structural members and base isolators were also considered in time history analysis. The obtained results indicate that demand estimates of fixed-base models are significantly higher than that of base-isolated models for superstructure as expected. Total lateral

displacements are higher in base-isolated models, but significant part of demands is absorbed at isolator interface and transmitted demands are at negligible levels in almost all considered cases. System behavior also varies according to the type of isolator used. It is seen that LRB type isolators are the most effective isolators in damping the demands. Since FS type isolators cannot generate recall force, LRB + FS type isolators are subjected to considerably higher demands compared to LRB type isolators. For this reason, the ratio of FS type isolators in LRB + FS combined models is very important parameter in design stage and their careful examination is required. However, none of LRB + FS models exceeded limit states for the same target design displacement values in this study. Therefore, using LRB and FS type isolators together can be preferred for economic reasons. The main advantage of FPS type isolators is their ability to produce self-centering force. This property can be a very important parameter in base isolation systems with large lateral displacement demands, especially for asymmetrical buildings, although their seismic demands are considerably higher than that of LRB type isolators. This study shows that LRB type isolators seem to be a better choice for regular buildings that have not re-centering problem.

Authors' contributions Authors' contribution is equal.

Funding No funding was received for conducting this study.

Declarations

Ethics approval There is no conflict in this study.

References

AASHTO (2014) Guide specifications for seismic isolation design, 4th edn. American Association of State Highway and Transportation Officials, Washington

Almazán JL, De la Llera JC (2002) Analytical model of structures with frictional pendulum isolators. Proc the Earthq Eng Struct Dyn. https://doi.org/10.1002/eqe.110

ASCE/SEI 7-16 (2016) Minimum design loads and associated criteria for buildings and other structures. Reston: American Society of Civil Engineers

Cancellara D, De Angelis F (2019) Dynamic assessment of base isolation systems for irregular in plan structures: Response spectrum analysis vs nonlinear analysis. Compos Struct 215:98–115. https://doi.org/10.1016/j.compstruct.2019.02.013

Ceccoli C, Mazzotti C, Savoia M (1999) Non-linear seismic analysis of base-isolated RC frame structures. Earthq Eng Struct Dyn 28:633–653. https://doi.org/10.1002/(SICI)1096-9845(199906)28:6%3c633::AID-EQE832%3e3.0.CO,2-3

Constantinou MC, Whittaker AS, Kalpakidis Y, Fenz DM, Warn GP (2007) Performance of seismic isolation hardware under service and seismic loading [Report MCEER-07-0012]. Buffalo, NY

De Domenico D, Ricciardi G, Infanti S, Benzoni G (2019) Frictional heating in double curved surface sliders and its effects on the hysteretic behavior: an experimental study. Front Built Environ 5:74. https://doi.org/10.3389/fbuil.2019.00074

Deringol AH, Bilgin H (2018) Effects of the isolation parameters on the seismic response of steel frames. Earthq Struct 15(3):319–334. https://doi.org/10.12989/eas.2018.15.3.319

EN 1998-2 (2005) Eurocode 8: design of structures for earthquake resistance – Part 2: bridges. Brussels: European Committee for Standardization

Erduran E, Dao ND, Ryan KL (2011) Comparative response assessment of minimally compliant low-rise conventional and base-isolated steel frames. Earthq Eng Struct Dyn 40:1123–1141. https://doi.org/10.1002/eqe.1078

FEMA-P-450 (2003) Nehrp Recommended Provisions For Seismic Regulations For New Buildings and Other Structures. In, Washington DC, USA

FEMA-451B (2016) 2015 NEHRP Recommended Provision for New Buildings and Other Structures: Training and Instructional Materialsxamples In, Washington DC, USA

FEMA-P-751 (2012) 2009 NEHRP Recommended Seismic Provisions:Design Examples In, Washington DC, USA

FEMA-P-752 (2013) 2009 NEHRP Recommended Seismic Provisions:Training and Instruction Materials. Prepared by National Institute of Building Sciences and Building Seismic Safety Council for the Federal Emergency Management Agency. In, Washington DC, USA

FEMA-P-1051 (2016) 2015 NEHRP Recommended Seismic Provisions:Design Examples In, Washington DC, USA

Gandelli E, Penati M, Quaglini V, Lomiento G, Miglio E, Benzoni GM (2019) A novel OpenSees element for single curved surface sliding isolators. Soil Dyn Earthq Eng 119:433–453. https://doi.org/10.1016/j.soildyn.2018.01.044

Ghasemi M, Talaeitaba SB (2020) On the effect of seismic base isolation on seismic design requirements of RC structures. Structures 28:2244–2259. https://doi.org/10.1016/j.istruc.2020.09.063

Giammona AP, Ryan KL, Dao ND (2015) Evaluation of assumptions used in engineering practice to model buildings isolated with triple pendulum isolators in SAP2000. Earthq Spectra 31(2):637–660. https://doi.org/10.1193/090213EQS242M

Güner G (2012) Bir Hastane Yapısının Klasik Yöntemle Ve Sismik İzolatör Kullanılarak Tasarımının Dinamik Yönden Karşılaştırılmasının Yapılması. PhD Thesis. Institute of Science. İTU İstanbul Turkey (in Turkish)

Hall JF (2006) Problems encountered from the use (or misuse) of Rayleigh damping. Earthq Eng Struct Dyn 35:525–545. https://doi.org/10.1002/eqe.541

Heaton TH, Hall JF, Wald DJ, Halling MW (1995) Response of high-rise and base-isolated buildings to a hypothetical Mw 7.0 blind thrust earthquake. Science 267:206–211. https://doi.org/10.1126/science.267.5195.206

Ismail M (2015) Elimination of torsion and pounding of isolated asymmetric structures under near-fault ground motions. Struct Control Health Monit 22:1295–1324. https://doi.org/10.1002/stc.1746

Jangid R (2007) Optimum lead–rubber isolation bearings for near-fault motions. Eng Struct 29:2503–2513. https://doi.org/10.1016/j.engstruct.2006.12.010

Jangid R, Kelly J (2001) Base isolation for near-fault motions. Earthq Eng Struct Dyn 30:691–707. https://doi.org/10.1002/eqe.31

Kayhan AH, Korkmaz KA, Irfanoglu A (2011) Selecting and scaling real ground motion records using harmony search algorithm. Soil Dyn Earthq Eng 31:941–953. https://doi.org/10.1016/j.soildyn.2011.02.009

Kelly JM (2003) Tension buckling in multilayer elastomeric bearings. J Eng Mech 129:1363–1368. https://doi.org/10.1061/(ASCE)0733-9399(2003)129:12(1363)

Kilar V, Koren D (2009) Seismic behaviour of asymmetric base isolated structures with various distributions of isolators. Eng Struct 31:910–921. https://doi.org/10.1016/j.engstruct.2008.12.006

Kulkarni JA, Jangid R (2002) Rigid body response of base-isolated structures. J Struct Control 9:171–188. https://doi.org/10.1002/stc.11

Lomiento G, Bonessio N and Benzoni G (2012) Effects of loading characteristics on the performance of sliding isolation devices. In: 15th world conference on earthquake engineering. At: Lisbon, Portugal, 24–28 September 2012

Matsagar VA, Jangid R (2004) Influence of isolator characteristics on the response of base-isolated structures. Eng Struct 26:1735–1749. https://doi.org/10.1016/j.engstruct.2004.06.011

Matsagar V, Jangid R (2010) Impact response of torsionally coupled base-isolated structures. J Vib Control 16:1623–1649

Mazza F (2017) Lateral-torsional response of base-isolated buildings with curved surface sliding system subjected to near-fault earthquakes. Mech Syst Signal Process 92:64–85. https://doi.org/10.1016/j.ymssp.2017.01.025

Mazza F (2019) Effects of the long-term behaviour of isolation devices on the seismic response of base-isolated buildings. Struct Health Monit 26(4):e2331. https://doi.org/10.1002/stc.2331

Mazza F, Mazza M (2016) Nonlinear seismic analysis of irregular rc framed buildings base-isolated with friction pendulum system under near-fault excitations. Soil Dyn Earthq Eng 90:299–312. https://doi.org/10.1016/j.soildyn.2016.08.028

Mazza F, Mazza M (2017) Sensitivity to modelling and design of curved surface sliding bearings in the nonlinear seismic analysis of base-isolated rc framed buildings. Soil Dyn Earthq Eng 100:144–158. https://doi.org/10.1016/j.soildyn.2017.05.028

Mazza F, Mazza M, Vulcano A (2017) Nonlinear response of rc framed buildings retrofitted by different base-isolation systems under horizontal and vertical components of near-fault earthquakes. Earthq Struct 12:135–144. https://doi.org/10.12989/eas.2017.12.1.135

Mazza F, Mazza M, Vulcano A (2018) Base-isolation systems for the seismic retrofitting of rc framed buildings with soft-storey subjected to near-fault earthquakes. Soil Dyn Earthq Eng 109:209–221. https://doi.org/10.1016/j.soildyn.2018.02.025

McVitty WJ, Constantinou MC (2015) Property modification factors for seismic isolators: Design Guidance for Buildings. MCEER report 15-0005

Meral E (2021) Determination of seismic isolation effects on irregular RC buildings using friction pendulums. Structures 34:3436–3452. https://doi.org/10.1016/j.istruc.2021.09.062

Mokha A, Constantinou M, Reinhorn A (1993) Verification of friction model of Teflon bearings under triaxial load. J Struct Eng 119:240–261. https://doi.org/10.1061/(ASCE)0733-9445(1991)117:4(1201)

Mokha A, Constantinou M, Reinhorn A, Zayas VA (1991) Experimental study of friction-pendulum isolation system. J Struct Eng 117:1201–1217. https://doi.org/10.1061/(ASCE)0733-9445(1991)117:4(1201)

Naeim F, Kelly JM (1999) Design of seismic isolated structures: from theory to practice. John Wiley and Sons

New Zealand Society for Earthquake Engineering (NZSEE) (2019) Guideline for the Design of Seismic Isolation Systems for Buildings. www.nzsee.org.nz/publications/design-of-seismic-isolation-systems-for-buildings

Ordonez D, Foti D, Bozzo L (2003) Comparative study of the inelastic response of base isolated buildings. Earthq Eng Struct Dyn 32:151–164. https://doi.org/10.1002/eqe.224

Ozer E, Inel M, Cayci BT (2022) Seismic behavior of LRB and FPS type isolators considering torsional effects. Structures 37:267–283. https://doi.org/10.1016/j.istruc.2022.01.011

Ozdemir G, Bayhan B (2015) Response of an isolated structure with deteriorating hysteretic isolator model. Res Eng Struct Mat 1(1):1–9. https://doi.org/10.17515/resm2014.01st1216

Ozmen HB (2017) Developing hybrid parameters for measuring damage potential of earthquake records: case for RC building stock. Bull Earthq Eng 15:3083–3101. https://doi.org/10.1007/s10518-016-0080-8

Ozmen HB, Inel M, Akyol E et al (2014) Evaluations on the relation of RC building damages with structural parameters after May 19, 2011 Simav (Turkey) earthquake. Nat Hazards 71:63–84. https://doi.org/10.1007/s11069-013-0900-y

Ozmen HB, Yilmaz H, Yildiz H (2019) An acceleration record set for different frequency content, amplitude and site classes. Res Eng Struct Mater 5(3):321–333. https://doi.org/10.17515/resm2019.116ea0209ds

Pacific Earthquake Engineering Research Center (PEER) (2019) Ground Motion Database. Available at: http://ngawest2.berkeley.edu/(2019). Accessed 19.05.2019

Panchal VR, Jangid RS (2009) Seismic response of structures with variable friction pendulum system. J Earthq Eng 13(2):193–216. https://doi.org/10.1080/13632460802597786

Ryan KL, Kelly JM, Chopra AK (2005) Nonlinear model for lead–rubber bearings including axial-load effects. J Eng Mech 131:1270–1278. https://doi.org/10.1061/(ASCE)0733-9399(2005)131:12(1270)

Ryan KL, Polanco J (2008) Problems with rayleigh damping in base-isolated buildings. J Struct Eng 134:1780–1784. https://doi.org/10.1061/(ASCE)0733-9445(2008)134:11(1780)

SAP (2000) CSI (2020) Integrated software for structural analysis and design. Computers and Structures Inc., Berkeley USA

SEMAp Sargı Etkisi Modelleme Analiz Programı (2008) Tubitak Proje No: 105M024 Ankara, Turkey (in Turkish)

Seranaj A, Garevski M (2018) The required ductility reduction of soft storey buildings through application of base isolation. Res Eng Struct Mat 4(1):49–60. https://doi.org/10.17515/resm2016.78ea0726

Soni DP, Mistry BB, Jangid RS, Panchal VR (2011) Seismic response of the double variable frequency pendulum isolator. Struct Cont and Health Monit 18(4):450–470. https://doi.org/10.1002/stc.384

Şengel HS, Hakan E, Yavuz E (2009) Sismik İzolasyon Tekniği ve Kullanılışına İlişkin Örnek Uygulama. J Eng Arch Fac Eskiseh Osmangazi Univ 22:165–178

Sharbatdar M, Vaez SH, Amiri GG, Naderpour H (2011) Seismic response of base-isolated structures with LRB and FPS under near fault ground motions. Proc Eng 14:3245–3251. https://doi.org/10.1016/j.proeng.2011.07.410

Tena-Colunga A, Escamilla-Cruz JL (2007) Torsional amplifications in asymmetric base-isolated structures. Eng Struct 29:237–247. https://doi.org/10.1016/j.engstruct.2006.03.036

Tena-Colunga A, Zambrana-Rojas C (2006) Dynamic torsional amplifications of base-isolated structures with an eccentric isolation system. Eng Struct 28:72–83. https://doi.org/10.1016/j.engstruct.2005.07.003

Turkish Building Earthquake Code (TBEC-2018) (2018) Republic of Turkey Prime Ministry Disaster and Emergency Management Authory Presidential of Earthquake Department. Ankara, Turkey (in Turkish)

Turkey Earthquake Risk Map (TERM) (2018) Republic of Turkey Prime Ministry Disaster and Emergency Management Authory Presidential of Earthquake Department. Ankara, Turkey https://tdth.afad.gov.tr. Accessed 08.09.2019

Vaez SH, Naderpour H, Kalantari S, Fakharian P (2012) Proposing the Optimized Combination of Different Isolation Bearings Subjected to Near-Fault Ground Motions. 15th World Conference on Earthquake Engineering At: Lisbon, Portugal, 24–28 September 2012

Whittaker D (2016) Seismic Isolation-A structural engineer's comparison of lead-rubber versus curved-surface-slider type isolation bearings. In Proceedings of the NZSEE Conference, Christchurch, 1 – 3 April 2016, New Zealand

Wu YM, Samali B (2002) Shake table testing of a base isolated model. Eng Struct 24:1203–1215. https://doi.org/10.1016/S0141-0296(02)00054-8

Yao M, Li TY (2012) Isolated structures research and comparative with traditional seismic structures. Adv Mat Res. https://doi.org/10.4028/www.scientific.net/AMR.594-597.1734

Zayas VA, Mahin SA (1987) The FPS earthquake resisting system experimental report, Earthquake Engineering Research Center

Springer Nature or its licensor holds exclusive rights to this article under a publishing agreement with the author(s) or other rightsholder(s); author self-archiving of the accepted manuscript version of this article is solely governed by the terms ofsuch publishing agreement and applicable law.